# Polymer Chemistry

Accepted Manuscript






ROYAL SOCIETY OF CHEMISTRY

www.rsc.org/polymers

Cite this: DOI: 10.1039/c0xx00000x

www.rsc.org/xxxxxx

ARTICLE TYPE

# $CO_2$-induced reversible morphology transition from giant worms to polymersomes assembled from a block-random segmented copolymer

**Wei Wang,[a,c] Hanbin Liu,[a,c] Meng Mu,[a,c] Hongyao Yin[a,c] and Yujun Feng*[a,b]**

***Received (in XXX, XXX) Xth XXXXXXXXX 20XX, Accepted Xth XXXXXXXXX 20XX***

**DOI: 10.1039/b000000x**

Well-defined block copolymers represent "stars" among amphiphilic compounds for self-assemblies. However, few studies have been addressed on their block-random "hybrid" counterparts. In this work, a segmented diblock copolymer containing one random block, $PEO_{113}$–*b*–P($4VP_{90}$–*r*–$DEAEMA_{30}$), was prepared via RAFT technique from the hydrophilic poly(ethylene oxide) block and random hydrophobic block copolymerized from 2-(diethylamino)ethyl methacrylate (DEAEMA) and 4-vinyl pyridine (4VP). It was found that the copolymer in aqueous media could self-assembly into vesicles firstly, which then fuse hierarchically into giant wormlike micelles similar to shish kebab, with length and diameter of ca. 15 $\mu$m and 215 nm, respectively. After bubbling $CO_2$ into the copolymer solution up to saturation (pH 5.43), the giant worms transform into polymersomes with a diameter about 75 nm which is much larger than that of the spherical micelles assembled from the same polymer treated with HCl (pH 3.32). The vesicles obtained could restore back to wormlike aggregates after depleting $CO_2$ by $N_2$. Protonation-deprotonation of the PDEAEMA unit, as well as the intensive steric hindrance effect from the adjacent 4VP groups, hydrogen bonding between different 4VP units and free $H_2O$ in the interior of polymersomes, are accounted for such a $CO_2$-driven reversible morphology transition.

## Introduction

Since the pioneering work on self-assembly of well-defined block copolymers in solution appeared early 1990s,[1] tremendous developments in this field have been achieved,[2] not only out of their unique microstructures, but also because of their fascinating macroscopic properties to furnish them into practical supramolecular materials[3] or "smart" nano-objects.[4]

Among the various assembly morphologies, polymersomes (vesicles formed from polymers),[5] are most attractive as they are archetypes of the self-assemblies from biological amphiphilies and show superior properties to low-molecular-weight liposomes, thus find diversified end uses,[6,7] particularly as an ideal drug delivery vehicle.

Since many potential applications require the ability to control the release of substances encapsulated in the interior compartment and/or in the hydrophobic core of membrane, intelligent polymersomes whose morphological transitions are interchangeable between polymersome and other microstructures upon triggering by a specific stimulus emerged recently.[8] The regulation of polymer vesicles can mimic and investigate some organismal behaviours such as volume tuning, unfolding and endocytosis, which would be helpful for us to understand biological autonomous motions in nature.[9] Moreover, morphology transition of copolymer self-assemblies induced by external stimuli provides greater envisions for sensing applications and controlled release,[10] drug delivery,[11] enzymatic nano-reactors,[12] and pharmaceutical technology,[13] to name just a few.

Generally, the transition from polymer vesicles to other morphologies can be tuned by an external physical or chemical stimulating signal such as pH,[14] temperature,[15] light,[16] redox,[17] and electrical field,[18] etc, to afford controlled release of encapsulated drugs,[10] functional materials,[19] and bio-imaging.[20] Grubbs's group[21] and Jiang *et al.*[22] realized a morphological transition from spherical micelle to vesicle with increasing temperature or irradiating by UV. Besides, Discher's team[23] and Hubbell *et al.*[17] observed a shift from vesicles to wormlike micelles upon pH-inducement or oxidation-stimulation. But noteworthily, to our knowledge, the transformation from polymer worms to vesicles is less documented, and the trigger pH has been topping on the stimulus list for the existence of the numerous pH gradients in both normal and pathophysiological states of some biological systems.[24] However, alternate addition of acid and base to adjust pH would result in residue accumulation, and the system may be contaminated or weakened to sense the stimulation.[25] Therefore, it is highly desirable to explore a more environmental-benign trigger possessing a suitable switchable mode.

$CO_2$ is just such a mild trigger due to its feeble acidity and metabolite character in cells. Besides, $CO_2$ as a trigger is easily-removing and free of contamination because of the produced bicarbonate salt is unstable, thus endowing the system with a better "smart" reversibility.[26] Most importantly, $CO_2$ possesses a good biocompatibility and membrane permeability as an endogenous metabolite, thus leading to a great potential application in biotherapy.[27] In such a context, Yuan's team[28] developed vesicles based on a diblock copolymer composed of polyethylene glycol (PEO) and $CO_2$-responsive poly(*N*-amidino) dodecyl acrylamide (PAD), and found the vesicles could undergo an interesting "breathing" behavior upon $CO_2$ stimuli—the hydrodynamic radius change reversibly between 59 and 120 nm. Soon later, Zhao and coworkers[9,27,29] extended $CO_2$-stimulated

diversiform deformations such as polymer vesicles to large sacs *via* triblock terpolymer PEO–*b*–PS–*b*–PDEAEMA, and polymeric microtubules to polymersomes or vesicles and further to spherical micelles based on PEO–*b*–PAD–*b*–PS, in which PDEAEMA and PAD are protonated when continuously purging with $CO_2$. So the requisition of optimizing interfacial free energy drives shape transformation. But it is worth pointing out that all the above assemblies are based on well-defined block copolymers, which involved a relatively tedious and time-consuming synthesis processes, requiring fine control of multi-step copolymerization and post-polymerization treatment.

Random copolymers, on the contrary, could be achieved from diverse components in a single polymerization step,[30] and the random strategy might render a special morphology. Eisenberg and coworkers[31] observed bowl-shape aggregates assembled from the sole random copolymer PS–*co*–PMAA, and they found such assemblies may result from the hydrogen bond interactions among carboxylate groups along the backbone, implying both polymer composition and architecture play important roles on the micellar morphology. The same team[32] then extended their work by mixing a random copolymer PS–*co*–PMAA in the solution of well-defined diblock copolymer PS–*b*–PAA, and found that with increasing MAA content, the localization of the random copolymer in the aggregates changed from the core to the interface, which led to a morphological transition from sphericals to vesicles; while the random copolymer was the minor component in the mixture, vesicles were formed with the random copolymer preferentially at the interface; when the random copolymer was the major component in the mixture, large sphericals could be formed with the block copolymer serving as a surfactant. Aggregates with both rod and vesicle morphologies were observed for random copolymers with a high molar mass at low water contents; otherwise, only vesicles were seen. Tsitsilianis *et al.*[33,34] recently demonstrated a strategy to prepare the so-called segmented polymers which bear at least a random copolymer as the building block by replacing a homopolymer block in the conventional diblock copolymer with a random one, and they found further tuning of the copolymer properties can be achieved through such a block-random topology. Enlightened by this concept, we prepared two structurally-similar and molecular-weight-equal terpolymers—one is a completely block terpolymer, $PEO_{45}$–*b*–$PSt_{66}$–*b*–$PDEAEMA_{90}$, while another one, $PEO_{45}$–*b*–P($St_{66}$–*r*–$DEAEMA_{93}$), possesses only two blocks, the second of which is a random copolymer composed of styrene and DEAEMA.[35] Both polymers can form polymersomes before $CO_2$ treatment, but the vesicles resulted from triblock copolymer do not change after uptaking $CO_2$; instead, the vesicles from the diblock copolymer would transfer into spherical micelles after reaction with $CO_2$, but the spherical micelles cannot reversibly return back to vesicles. Such a new finding from block-random segmented copolymer stimulated our interest to further explore morphology transition based on vesicles with alternate treatment of $CO_2$ and $N_2$, and to see if other segments can get similar results.

To this end, the styrene unit in above PEO–*b*–P(St–*r*–DEAEMA) was replaced in this work by 4-vinyl pyridine (4VP) to get a new block-random "hybrid" copolymer because P4VP could form hydrogen bond with water, which may bring about new findings. This diblock copolymer was prepared from reversible addition-fragmentation chain transfer (RAFT) polymerization, and the morphological transition of the polymer assemblies triggered by $CO_2$ was investigated. It was found that the copolymer could self-assemble into giant wormlike micelles by fusing vesicles in aqueous solution without $CO_2$, but the worms would transform into polymersomes after the aeration of $CO_2$, and could restore to threadlike aggregates again when $CO_2$ was depleted from the solution.

## Experimental

### Materials

The monomers, 2-(diethylamino)ethyl methacrylate (DEAEMA, Aldrich, 99%) and 4-vinyl pyridine (4VP, Sigma-Aldrich, ≥99%), were passed through an activated basic alumina column to eliminate the inhibitors. Poly(ethylene glycol) methyl ether (PEO, $M_n$ ~5,000 g $mol^{-1}$), 4,4-azobis(4-cyanovaleric acid) (ACVA, ≥98.0%) , 4-(dimethylamino) pyridine (DMAP, ≥99%), and *N*-(3 dimethylaminopropyl)-*N′*-ethylcarbodiimide hydrochloride crystalline (EDAC), were purchased from Sigma-Aldrich and used as received. The chain transfer agent (CTA), 4-cyano-4-thiothiopropylsulfanylpentanoic acid (CTPPA) was synthesized according to a previously-reported procedure.[36] The organic solvents with A.R. grade were obtained from Guanghua Sci-Tech Co., Ltd. (Guangdong, China) without further treatment unless otherwise specified. The deionized water (conductivity, $\kappa$ = 7.9 $\mu S \cdot cm^{-1}$) used in the dialysis process was treated by the ultrapure water purification system (CDUPT-Ⅲ, Chengdu Ultrapure Technology Co., Ltd., China). The $CO_2$ and $N_2$ gas with a purity of above 99.99% were provided by the Jinnengda Gas Company (Chengdu, China).

### Characterization

$^1$H NMR spectra were carried out at 25 °C on a Bruker AV300 NMR spectrometer at 300 MHz, and the chemical shifts (δ) are presented in parts per million (ppm) with reference to the internal standard protons of tetramethylsilane (TMS).

The molecular weight (MW) and the molecular weight distribution (MWD) of the polymer were determined by a HLC-8320 gel permeation chromatography system (TOSOH, Japan) equipped with TSK gel super HZM-M 6.0×150 mm and TSK gel SuperHZ3000 6.0×150 mm chromatographic column, as well as a refractive index detector. THF was selected as the eluent at a flow rate of 1.0 mL $min^{-1}$ at 40 °C. Monodisperse polystyrene was used as the standard to build the calculation curve.

Transmission electron microscopy (TEM) observation was conducted on a Hitachi H600 electron microscope at an acceleration voltage of 75 kV. The specimens were prepared by dipping about 15 $\mu$L micellar solution on a copper grid coated with polyvinyl formal film and then stained with 0.2wt% phosphotungstic acid aqueous solution for 20–30 s followed by drying in air.

Fluorescence microscopy (FM) images were recorded with a Leica TCS SP8 (Leica, Germany) confocal laser scanning microscope at 570–620 nm (excitation at 552 nm) with an HCX PL APO 63×1.4 oil immersion objective. The sample is prepared as follows: 500 $\mu$L polymer solution was taken in an eppendorf tube, then 10 $\mu$L of 0.02 mM fluorescent dye (PKH26, Sigma) was added, and they were then gently mixed. Finally 10 $\mu$L of

this mixture solution was placed on a glass slide, followed by drying in a vacuum oven and then washed with deionized water.

Dynamic light scattering (DLS) measurements were performed with Malvern Zetasizer Nano-ZS90. He-Ne laser with a wavelength of 633 nm was used. The temperature was set to 25 °C and the scattering angle is fixed at 90°.

The pH variation was monitored by a Sartorius basic pH meter PB-10 (± 0.01) calibrated with standard buffer solutions. The conductivity of micellar solution was determined by an FE30 conductometer (Mettler Toledo, USA). Both measurements were conducted at 25 °C.

### Synthesis of the macromolecular chain transfer agent *macro*-$PEO_{113}$

The macromolecular chain transfer agent, *macro*-$PEO_{113}$, was prepared following the procedure reported previously.[36] Dichloromethane ($CH_2Cl_2$) was dried with $CaH_2$ and then refluxed to be used as the solvent for the reaction. The detailed process could be described as follows: chain transfer agent CTPPA (0.554 g, 2.0 mmol), mPEG-5000 (5.003 g, 1.0 mmol), EDAC (0.767 g, 4.0 mmol) and DMAP (0.244 g, 2.0 mmol) were dissolved in 50 mL dry $CH_2Cl_2$, and then transferred into a round bottom flask stirred for 48 h at room temperature after deoxygenating by bubbling Ar gas for 15 min. The reaction mixture was precipitated in −72 °C *n*-hexane (in the bath of acetone and dry ice mixture) three times, and then washed with diethyl ether three times. Finally, yellow powder was obtained after lyophilisation (4.802 g, yield: 96%). $^1$H NMR (δ, ppm, $CDCl_3$; Fig. 1): 3.62 (−C**H**$_2$C**H**$_2$O−), 3.36 (−OC**H**$_3$, −SC**H**$_2$−), 2.38−2.71 (−OOCC**H**$_2$C**H**$_2$−), 1.85 (−C(C**H**$_3$)(CN)−), 1.67−1.85 (−SCH$_2$C**H**$_2$CH$_3$), 0.97−1.02 (−SCH$_2$CH$_2$C**H**$_3$). The molecular weights are $M_{n,NMR}$ = 5,277 g·mol$^{-1}$, $M_{n,GPC}$ = 5,521 g·mol$^{-1}$, and $M_w/M_n$ = 1.03.

### Synthesis of the block-random segmented copolymer $PEO_{113}$−*b*−($4VP_{90}$−*r*−$DEAEMA_{30}$)

Starting with the RAFT agent *macro*-$PEO_{113}$, the diblock copolymer $PEO_{113}$-*b*-($4VP_{90}$-*r*-$DEAEMA_{30}$) was synthesized as follows: the *macro*-$PEO_{113}$ (0.301 g, 0.058 mmol), 4VP (1.271 g, 12.08 mmol), DEAEMA (2.351 g, 12.69 mmol), ACVA (2.0 mg, 0.0072 mmol) and 3.5 mL dry THF were added into a reaction tube equipped with a magnetic bar. The mixture reacted at 70 °C for 24 h under magnetic stirring after deoxygenizing by three freeze-pump-thaw cycles. $^1$H NMR (δ, ppm, $CD_3OD$; Fig. 1): 6.58−7.36, 8.05−8.58 (−C$_5$**H**$_4$), 3.60 (−C**H**$_2$C**H**$_2$O−), 3.75−4.19 (−COOC**H**$_2$CH$_2$N(CH$_2$CH$_3$)$_2$), 2.21−2.87 (−OOCC**H**$_2$C**H**$_2$−, −COOCH$_2$C**H**$_2$N(C**H**$_2$CH$_3$)$_2$, −C**H**CH$_2$C$_5$H$_4$), 1.24−2.10 (−C(C**H**$_3$)CH$_2$−, −CC**H**$_3$CNCH$_2$−, −SCH$_2$C**H**$_2$CH$_3$), 0.35−1.20 (−N(CH$_2$C**H**$_3$)$_2$, −CCH$_3$C**H**$_2$−, −SCH$_2$CH$_2$C**H**$_3$, −C**H**$_2$CH−). From the peak area ratio of $PEO_{113}$ to DEAEMA moieties (peaks *b* and *h*, the bottom spectrum in Fig. 1), as well as the 4VP segment (peak *l*, Fig. 1) on the $^1$H NMR spectrum of the copolymer, the $M_n$, the polymerization degree (DP), of the polymer can be calculated via the following equations:

$$\frac{\delta_c}{4}:\frac{\delta_a}{2}:\frac{\delta_d}{2}=DP_{PEO}:DP_{PVP}:DP_{DEAEMA} \quad (1)$$

$$\frac{\delta_c}{4}=113 \quad (2)$$

where δ represents integral proportion, DP refers to polymerization degree, and the subscripts refer to different peak and units. The polymerization degree of two monomers in the random block are found to be $DP_{DEAEMA,NMR}$ = 30 and $DP_{4VP,NMR}$ = 90, respectively. The corresponding molecular weights are: $M_{n,NMR}$ = 20,295 g·mol$^{-1}$, $M_{n,GPC}$ = 22,156 g·mol$^{-1}$, and $M_w/M_n$ = 1.36.

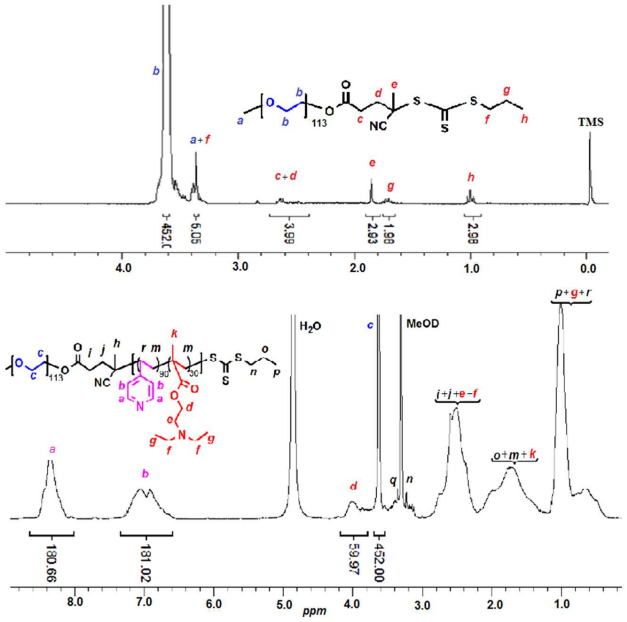


**Fig. 1** $^1$H NMR spectra of *macro*–$PEO_{113}$ in $CDCl_3$ (on the top) and $PEO_{113}$−*b*−($4VP_{90}$−*r*−$DEAEMA_{30}$) in $CD_3OD$.

### Preparation of micellar solution

40 mg polymer powders were dissolved in 10 mL THF, which is a good solvent for all the three units, followed by stirring for several hours to ensure the polymer to be dissolved completely. Then the obtained polymer solution was transferred to a dialysis bag (MW cut-off: 8,000−14,000 g·mol$^{-1}$) and dialyzed against deionized water for 3−4 days to exclude the organic solvent. After that, the micellar solution was diluted to 20 mL, yielding a micellar solution with concentration of 2 g·L$^{-1}$. Such final micellar solution was used for all the further experiments including conductivity and pH monitoring, $CO_2$-responsiveness, as well as TEM and FM observation.

## Results and discussion

Unlike the covalent link of a homopolymer and a random block copolymer proposed by Tsitsilianis *et al.*,[33] here in this work, macromolecular chain transfer agent (*macro*-$PEO_{113}$) was prepared the first, with which the other two monomers (4VP and DEAEMA) further copolymerization happened to form a random copolymer which co-acts as the second block through RAFT copolymerization (Scheme 1). According to Liu *et al.*,[35] the reactivity ratio of styrene to DEAEMA was 0.22:0.42, and here 4VP possesses a structure similar to styrene except the more prominent electron-donator effect. Therefore, 4VP and DEAEMA would be randomly distributed in the second block.

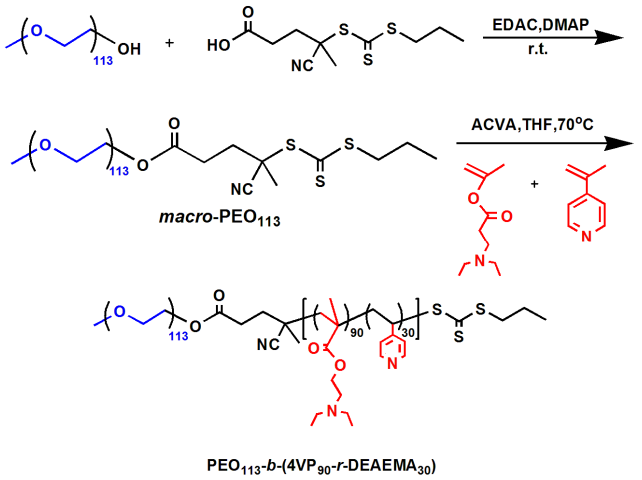


**Scheme 1** The synthesis pathway of the block-random segmented polymer $PEO_{113}$-*b*-P($4VP_{90}$-*r*-$DEAEMA_{30}$).

As aforementioned, the $M_n$ of the copolymer from $^1H$ NMR is comparable to that from GPC; the polydispersity is 1.36, less than 1.40 and could be accepted for a controlled living radical polymerization.[37] What is more, as reported by Eisenberg,[38] the MWD determined by GPC for the copolymer containing 4VP or DEAEMA should be broader than the real polydispersity because some 4VP or DEAEMA units would have an adsorption in the GPC column, which introduces a systematic error into the retention time measurement. Meanwhile, as shown in Fig. 2, the GPC curve of the copolymer has a shift compared with *macro*-$PEO_{113}$, implying the complete initiation of *macro*-$PEO_{113}$ as a chain transfer agent and the success of the synthesis.

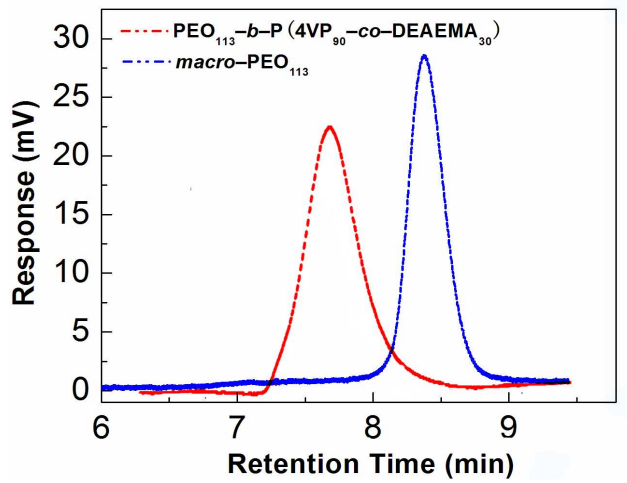


**Fig. 2** Comparison of GPC traces for the copolymer $PEO_{113}$–*b*–P($4VP_{90}$–*r*–$DEAEMA_{30}$) and RAFT agent *macro*-$PEO_{113}$.

The solubility parameters of PEO, P4VP, THF and $H_2O$ are 20.2, 20.6, 19.4 and 47.3 $MPa^{1/2}$, respectively, and the polymer-solvent interaction parameters, $\chi_{P4VP\text{-}THF}$ (0.3875) and $\chi_{PEO\text{-}THF}$ (0.3611), are very close,[39] though, the non-protonated P4VP segment is not soluble and hydrophobic in aqueous media;[38,40] without $CO_2$ treatment, PDEAEMA is also hydrophobic. Therefore, the amphiphilic $PEO_{113}$–*b*–P($4VP_{90}$–*r*–$DEAEMA_{30}$) could self-assemble into micelles with the block P($4VP_{90}$–*r*–$DEAEMA_{30}$) as the core and PEO as the shell. In THF, a good solvent for both blocks, the copolymer could be dispersed molecularly; however, unique microstructure would be expected after dialyzing against deionized water followed by equilibration for 3 days.

To prove this, morphological observation by TEM was performed. Surprisingly, as displayed in Fig. 3a, long filament-like or large linear wormlike structures are observed. Usually, the typical surfactant-based wormlike micelles have diameter of 1~10 nm and length of 10~$10^4$ nm,[41] and the polymer-based wormlike micelles possess diameter less than 100 nm;[42] nevertheless, the worms observed here have diameter around 215 nm and maximum contour length up to 15 $\mu$m, both of which are much larger than those of the traditional wormlike micelles.

Generally, the polymer micellar morphologies can be predicted by the hydrophilic mass fraction ($f$) of the copolymer:[6] a copolymer with $f_{philic}$ greater than 50% will self-assemble into traditional spherical micelles; with $f_{philic}$ between 40% and 50%, cylindrical or worm micelles are formed; when $f_{philic}$ is below 40%, vesicles may appear. Here, the $f_{philic}$ can be expressed as

$$f_{philic} = \frac{M_{PEO}/\rho_{PEO} + M_{DEAEMA^+}/\rho_{DEAEMA^+}}{M_{PEO}/\rho_{PEO} + M_{DEAEMA}/\rho_{DEAEMA} + M_{4VP}/\rho_{4VP}} \quad (3)$$

where the $M_{PEO}$, $M_{DEAEMA^+}$, $M_{DEAEMA}$, and $M_{4VP}$ are the molecular weight of PEO, charged DEAEMA, total DEAEMA, and 4VP; $\rho_{PEO}$, $\rho_{DEAEMA^+}$, $\rho_{DEAEMA}$, and $\rho_{4VP}$ are their corresponding density. According to Zhao's report,[9] $\rho_{PEO}$ = 1.15 g·$cm^{-3}$, $\rho_{4VP}$ = 0.989 g·$cm^{-3}$, $\rho_{DEAEMA^+} \approx \rho_{DEAEMA}$ =1.19 g·$cm^{-3}$, so the calculated $f_{philic}$ of $PEO_{113}$–*b*–P($4VP_{90}$–*r*–$DEAEMA_{30}$) is 23.3%, corresponding to the formation of vesicles other than wormlike micelles. Besides, few literature results show wormlike micelles with radius of hundreds of nanometre. So how the filament-like structures are formed?

If we closely look at the enlarged linear worms shown in Figs. 3b and 3c, it is clear that the long giant worms are connected by the vesicles continuously, with a clear contrast between the dark periphery and hollow centre (indicated by the arrows), looking like a necklace composed pearls, or more alike a bunch of shish kebab. The size of such a single vesicle was approximately 275 nm, much larger than that of the spherical micelles whose size is usually below 100 nm. Kressler *et al.*[43] observed similar wormlike polymersomes aggregates from a block-graft copolymer, poly(glycerol adipate)–*g*–(poly(3-caprolactone)–*b*–poly(ethylene oxide)), PGA–*g*–(PCL–*b*–PEO), and they attributed such an elongated fashion to the partially fused polymersomes under the influence of shear flow. Moreover, Liu *et al.*[44] illustrated that the stability of vesicles would increase after fusion due to the decrease of surface areas of vesicles and the increase of average density of hydrophilic segments on vesicles surfaces. Battaglia and coworkers[45] found vesicles formed by the diblcok copolymer polybutadiene-poly(methacrylic acid) become smaller with increasing pH until a transition to wormlike micelles at pH 8; they postulated the chains extend and swell caused the break-up of large vesicles to obtain smaller species of greater curvature, and then the vesicles subsequently collapse into pearl necklace-like structures, which eventually evolve into cylindrical micelles. Here in this system, therefore, it is possible that the vesicle wall composed of hydrophobic segment P(4VP–*r*–DEAEMA) would be inclined to merge together for greater curvature and higher average

hydrophilic density, which drive the vesicles to fuse after approaching to each other, and eventually to grow into giant wormlike micelles. So it is interesting to see what structure would appear when increasing the hydrophilcity of P(4VP–*r*–DEAEMA).

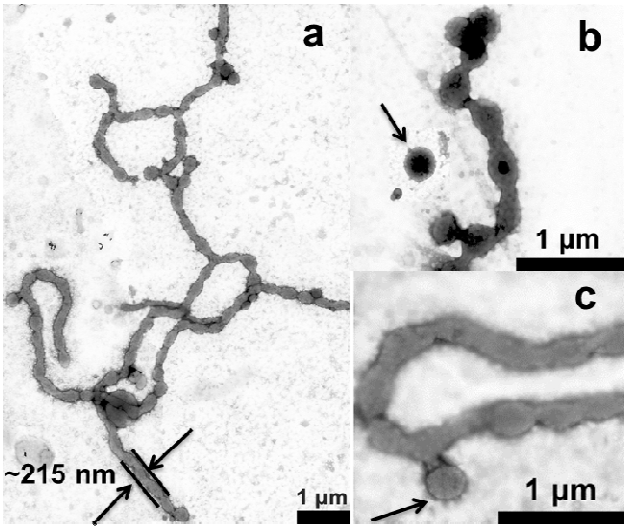


**Fig. 3** TEM (stained with 0.2 wt% phosphotungstic acid) images of polymer assemblies before $CO_2$ bubbling: (a) giant worms with a diameter about 215 nm; both (b) and (c) demonstrated large wormlike micelles are connected with fused vesicles (pointed by the black arrows).

What addressed above are the results obtained in the absence of $CO_2$; to explore the $CO_2$-stimuli responsiveness of the self-assemblies, the appearance and optical transmittance of the copolymer solution with and without $CO_2$ are compared. As displayed in the insets of Fig. 4, the original solution is absolutely opaque before $CO_2$ aeration, but it becomes transparent after 10 min of $CO_2$ treatment. Correspondingly, the transmittance varies from 0 to 84% during this period. It is well recognized that the turbidity of colloidal solution has a positive correlation with the colloidal size:[27] usually, the larger aggregates result in opaque solution, while the transparent solution implies self-assemblies with small size; thus, the gradual increase in transmittance here suggests that the size of the aggregates becomes smaller upon continuous $CO_2$ treatment.

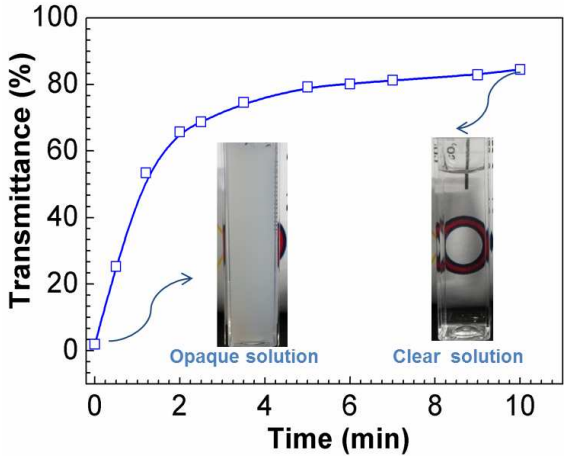


**Fig. 4** Changes in the appearance and transmittance of copolymer micellar solution with the $CO_2$ bubbling time. The transmittance was detected at the wavelength of 600 nm, and the polymer concentration is fixed at 2.0 g·L$^{-1}$.

With the uptake of $CO_2$, the variation of conductivity and pH of the polymer solution during alternate bubbling $CO_2$ and $N_2$ also confirm the responsiveness to $CO_2$. As shown in Fig. 5, the conductivity ($\kappa$) of polymer aqueous solution rises sharply from 55.6 to 186.6 $\mu$S·cm$^{-1}$ in 20 min, and finally ascends to the maximum during $CO_2$ bubbling, indicating the development of bicarbonate ions in solution.[46] Concurrently, the pH value drops from 7.50 to 5.43, suggesting the protonation of the tertiary amine groups in the DEAEMA unit. p*K*a determined by the continuous titration of 2.5 mL polymer solution with 2 mM hydrochloric acid was found to be 6.61. Following the previously-reported procedures[35,36] and based on the correlation between pH and p*K*a (the different pH values of the polymer solution as function of $CO_2$ bubbling time), the protonation degrees of DEAEMA moieties in copolymers at different pH values were calculated, which increases from 6.5% (it may result from the initial protonation of the DEAEMA unit by the $CO_2$ dissolved in water) to approximately 95% after 10-min $CO_2$ bubbling.

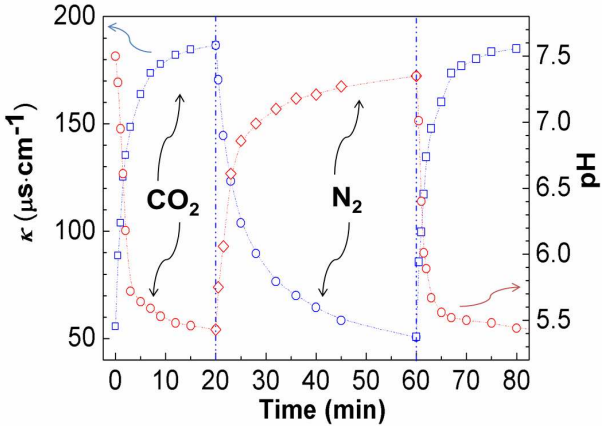


**Fig. 5** Changes in conductivity ($\kappa$) (blue curve, □ and ○) and pH (red curve, ○ and ◇) of copolymer solution with the alternate treatment of $CO_2$ and $N_2$. The measurements were conducted at room temperature with a fixed gas flow rate at approximately 15 mL·min$^{-1}$.

After inletting $CO_2$ at a flow rate approximately 15 mL·min$^{-1}$ for 30 min, the morphology was re-observed via TEM. As displayed in Fig. 6a, the giant worms have turned into polymersomes with an average diameter of about 70 nm, in good line with the DLS result which shows a hydrodynamic diameter about 75 nm with the polydispersity index (PDI) 0.20 (Fig. 7). In addition, as reported by Munk and Webber *et al.*,[40] the diblock polymer PEO–*b*–PVP would be hard to be protonated when the pH is higher than 5; and the reported p$K_a$ value of P4VP is around 4.7,[47] suggests that the P4VP would not be protonated when pH is higher than 4.7.[48] Thus stable micelles could be formed and the size will not change clearly at higher pH. Correspondingly, upon the aeration of $CO_2$, the pH would drop from 7.50 to 5.43 (with the prolongation of ventilation, the pH would not decline further), implying the pH of polymer solution would not go below 4.7

during $CO_2$ saturation. So we attribute such a morphology deformation to the protonation of DEAEMA segment. For comparison, the micellar solution at lower pH (3.32, much below the p$K_a$ of P4VP) which was adjusted by HCl was studied. The uniform spherical micelles with an average size of 35 nm were observed (Fig. 6b), and the average hydrodynamic radius $R_h$ was only 38 nm (Fig. 7). This means such a much lower pH (<<4.7) resulted from protonation of both DEAEMA and 4VP units, which make the copolymer more hydrophilic, thus the worms turning into spherical micelles instead of vesicles. Such a transition process indicates the weak acidic gas, $CO_2$, can drive large wormlike micelles to transform into polymersomes.

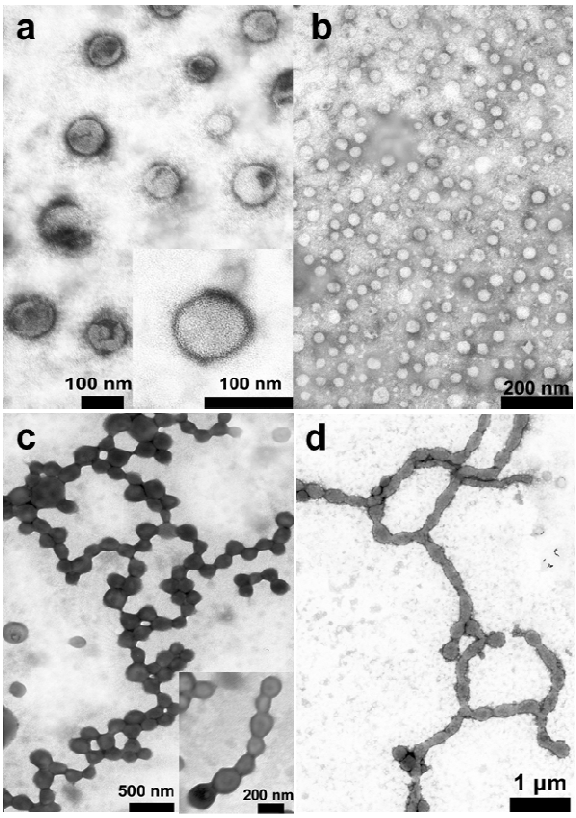


**Fig. 6** TEM images (stained with 0.2 wt% phosphotungstic acid) of (a) the assemblies treated with $CO_2$ to pH 5.43, (b) copolymer solution dealt with HCl to pH 3.32, (c) necklace-like aggregates after removing $CO_2$ by $N_2$ (pH=7.35), and (d) the giant worms before $CO_2$ treatment (pH=7.50).

To check if the morphology change is reversible, TEM observation was again performed on the $CO_2$-containing micellar solution re-treated by $N_2$. With extension of $N_2$ bubbling time, the transparent solution turns into opaque gradually (the transmittance drops from 84% to 4.85% in 40 min). As exhibited in Fig. 6c, these vesicles assemble into wormlike aggregates again. Even though these polymersomes did not revert back to regular worms, they were formed visibly by the connection of vesicles (the sample was black on account of staining for a longer time, but the wrinkles belong to vesicles and the size approaching 180 nm implies the microscopic structure may be formed by single vesicle). Moreover, this necklace-like structure was similar to the initial form, which verified that the morphology transition was invertible and manipulative.

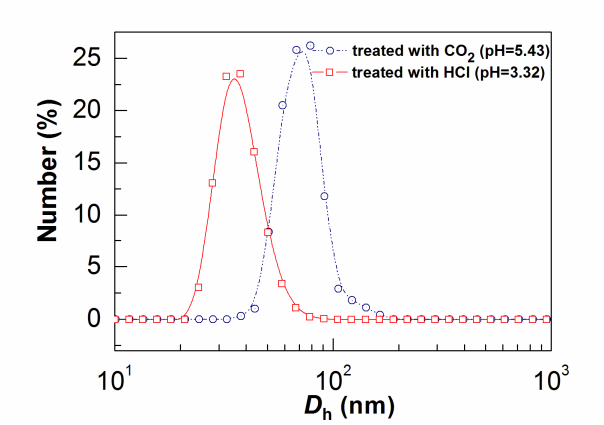


**Fig. 7** DLS data for micellar aggregates in the presence of $CO_2$ (pH=5.43) and the copolymer solution disposed with HCl (pH=3.32).

Due to the greater size of this polymer worms, the morphology changes of assemblies might be visualized by a fluorescence microscopy, which could give a broader view to see the full morphology. Since the fluorescence dye PKH26 was loaded into the self-assemblies without CO2 treatment by direct addition to the polymer solution, thus the red rod-like micelles appeared in Fig. 8a should be ascribed to the giant worms which have a contour length up to about 10 μm. Unfortunately, the polymersomes (obtained by treated with $CO_2$) were too small to be evidenced by microscope. However, when the $CO_2$ is discharged, short rod-like aggregates can be observed in light field (Fig. 8b), which was in consistent with the above necklace-like aggregates observed by TEM.

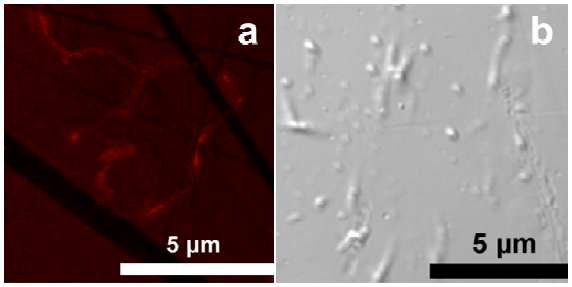


**Fig. 8** (a) Fluorescence microscopy images of giant worms before uptaking $CO_2$ and (b) photograph of micellar solution eliminated $CO_2$ by $N_2$ under light field.

Based on the above findings, we proposed the mechanism that how $CO_2$ induces the morphology change. Before $CO_2$ treatment, the segmented diblock copolymer possesses the hydrophobic random polymer segment P(4VP$_{90}$–*r*–DEAEMA$_{30}$) and a hydrophilic block PEO$_{113}$, which induce the micelles to form a hydrophilic-hydrophobic-hydrophilic three-layer structure (Scheme 2a) in aqueous solution. After reaction with $CO_2$, the DEAEMA moieties become protonated and covert into charged species, which would break the equilibrium of this system and drive the giant worms to turn into single polymersome. However, while aerating $N_2$ to eliminate $CO_2$, this system would have fewer charges and that may induce the single polymersome to return back to the initial state, in agreement with the theory of hydrophilic volume fraction, which forecasts the formation of

vesicles. With the aeration of $CO_2$, the polymer becomes more hydrophilic due to the protonation of DEAEMA units, which would drive the micellar morphology deformation in order to reduce the interfacial free energy originated from the electrostatic repulsion (Scheme 2b). In addition, the intensive steric hindrance effect from the adjacent 4VP groups in the random segment hinders the DEAEMA units to be protonated completely, and the random block also imparts hydrogen bond between 4VP units with free $H_2O$ in the interior of polymersomes[49] which increases the ability of water retention and also answers why giant worms do not transfer into traditional wormlike micelles or spherical micelles.

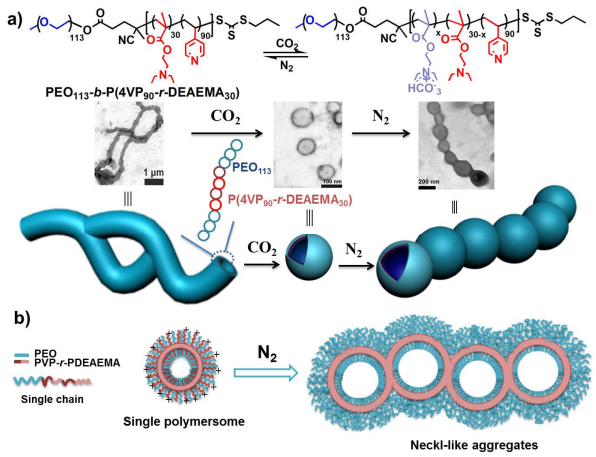


**Scheme 2** Schematic illustration of (a) protonation-deprotonation of the diblock copolymer $PEO_{113}$–*b*–$P(4VP_{90}$–*r*–$DEAEMA_{30})$ upon alternate treatment of $CO_2$ and $N_2$, and (b) the structure of polymersomes experienced $CO_2$ treatment formed by self-assembly of in water and the necklace-like aggregates formed by $N_2$ disposal.

## Conclusions

In short, long, linear giant worms have been assembled hierarchically through the fusion of vesicles formed by a block-random segmented diblock copolymer, and these filament structures are disassembled into polymersomes upon reaction with $CO_2$ at pH 5.43; on the contrary, only much smaller spherical micelles were got when decreasing the pH of polymer solution to 3.32 with HCl directly. When the $CO_2$ inside the polymer aqueous solution was depleted with $N_2$, the single vesicles would reform necklace-like aggregates. The hydrophilic volume fraction theory and the intensive steric hindrance effect from the adjacent 4VP groups, and hydrogen bonding between different 4VP units with free $H_2O$ molecules in the interior of polymersomes should be responsible for the morphology transformation. Considering the convenience of synthesis procedure of block-random segmented polymer, as well as the good biocompatibility and membrane permeability of $CO_2$ as a new trigger, the use of random copolymer as a tecton in the diblock copolymer possess huge potential applications in drug delivery, controlled release and biotherapy as well.

## Acknowledgements

The authors would like to thank the financial support from the National Natural Science Foundation of China (21273223, 21173207), and the Distinguished Youth Fund of Sichuan Province (2010JQ0029).

## Notes and references

[a] *Chengdu Institute of Organic Chemistry, Chinese Academy of Sciences, Chengdu 610041, P. R. China.*
[b] *Polymer Research Institute, State Key Laboratory of Polymer Materials Engineering, Sichuan University, Chengdu 610065, P. R. China. Tel. & Fax: +86 (0)28 8540 8037; E-mail: yjfeng@scu.edu.cn*
[c] *University of Chinese Academy of Sciences, Beijing 100049, P. R. China.*

1 M. Malmsten and B. Lindman, *Macromolecules*, 1992, **25**, 5440.
2 Y. Mai and A. Eisenberg, *Chem. Soc. Rev.*, 2012, **41**, 5969.
3 H. A. Klok and S. Lecommandoux, *Adv. Mater.*, 2001, **13**, 1217.
4 J. Rodriguez-Hernandez, F. Chécot, Y. Gnanou and S. Lecommandoux, *Prog. Poly. Sci.*, 2005, **30**, 691.
5 M. Antonietti and S. Förster, *Adv. Mater.*, 2003, **15**, 1323.
6 D. E. Discher and A. Eisenberg, *Science*, 2002, **297**, 967.
7 M.-H. Li and P. Keller, *Soft Matter*, 2009, **5**, 927.
8 (a) C. Ott, R. Hoogenboom, S. Hoeppener, D. Wouters, J. F. Gohy and U. S. Schubert, *Soft Matter*, 2009, **5**, 84; (b) A. Choucair and A. Eisenberg, *Eur. Phys. J. E*, 2003, **10**, 37; (c) K. Letchford and H. Burt, *Eur. J. Pharm. Biopham.*, 2007, **65**, 259.
9 Q. Yan and Y. Zhao, *J. Am.Chem. Soc.*, 2013, **135**, 16300.
10 J. Du and R. K. O'Reilly, *Soft Matter*, 2009, **5**, 3544.
11 (a) R. Haag, *Angew. Chem. Int. Ed.*, 2004, **43**, 278; (b) C. Allen, D. Maysinger and A. Eisenberg, *Colloid Surf. B-Biointerfaces*, 1999, **16**, 3
12 D. E. Discher and F. Ahmed, *Annu. Rev. Biomed. Eng.*, 2006, **8**, 323.
13 B. Lindman and P. Alexandridis, Amphiphilic block copolymers: self-assembly and applications, *Amsterdam: Elsevier Science Bv*, 2000.
14 (a) J. Du, Y. Tang, A. L. Lewis and S. P. Armes, *J. Am.Chem. Soc.*, 2005, **127**, 17982; (b) K. E. B. Doncom, C. F. Hansell, P. Theato and R. K. O'Reilly, *Polym. Chem.*, 2012, **3**, 3007.
15 (a) Y.Cai, K. B. Aubrecht and R. B. Grubbs, *J. Am.Chem. Soc.*, 2010, **133**, 1058; (b) A. O. Moughton and R. K. O'Reilly, *Chem. Commun.*, 2010, **46**, 1091.
16 (a) J.-F. Gohy, Y. Zhao, *Chem. Soc. Rev.*, 2013, **42**, 7117; (b) J. Li, M. Zhao, H. Zhou, H. Gao and L. Zheng, *Soft Matter*, 2012, **8**, 7858.
17 (a) A. Napoli, M. Valentini, N. Tirelli, M. Müller and J. A. Hubbell, *Nat. Mater.*, 2004, **3**, 183; (b) J.-H. Ryu, R. Roy, J. Ventura and S. Thayumanavan, *Langmuir*, 2010, **26**, 7086.
18 S. J. Lee and M. J. Park, *Langmuir*, 2010, **26**, 17827..
19 L.Zhai, *Chem. Soc. Rev.*, 2013, **42**, 7148.
20 M. S. Shim and Y. J. Kwon, *Adv. Drug. Deliver. Rev.*, 2012, **64**, 1046.
21 A. Sundararaman, T. Stephan and R. B. Grubbs, *J. Am.Chem. Soc.*, 2008, **130**, 12264.
22 X. K. Liu and M. Jiang, *Angew. Chem. Int. Ed.*, 2006, **45**, 3846.
23 Y. Geng, F. Ahmed, N. Bhasin and D. E. Discher, *J. Phys Chem. B.*, 2005, **109**, 3772.
24 Y. Bae, N. Nishiyama, S. Fukushima, H. Koyama, M. Yasuhiro and K. Kataoka, *Bioconjugate Chem.*, 2005, **16**, 122.
25 Q. Yan and Y. Zhao, *Chem. Commun.*, 2014, **50**, 11631.
26 (a) Z. Guo, Y. Feng, S. He, M. Qu, H. Chen, H. Liu, Y. Wu and Y. Wang, *Adv. Mater.*, 2013, **25**, 584; (b) Z. Guo, Y. Feng, Y. Wang, J. Wang, Y. Wu and Y. Zhang, *Chem Commun.*, 2011, **47**, 9348; (c) Y.

X. Liu, P. G. Jessop, M. Cunningham, C. A. Eckert and C. L. Liotta, *Scienc*e, 2006, **313**, 958.
27 Q. Yan and Y. Zhao, *Angew. Chem., Int. Ed.*, 2013, **52**, 9948.
28 Q. Yan, R. Zhou, C. K. Fu, H. J. Zhang, Y. W. Yin and J. Y. Yuan, *Angew. Chem., Int. Ed.*, 2011, **50**, 4923.
29 B. Yan, D. H. Han, O. Boissiere, P. Ayotte and Y. Zhao, *Soft Matter*, 2013, **9**, 2011.
30 (a) A. Honglawan, H. P. Ni, D. Weissman and S. Yang, *Polym. Chem*., 2013, **4**, 3667; (b) J. Guo, Y. Zhou, L. Qiu, C. Yuan and F. Yan, *Polym. Chem.*, 2013, **4**, 4004.
31 X. Liu, J. S. Kim, J. Wu and A. Eisenberg, *Macromolecules*, 2005, **38**, 6749.
32 X. Liu, J. Wu, J.-S. Kim and A. Eisenberg, *Langmuir*, 2006, **22**, 419.
33 C. Tsitsilianis, G. Gotzamanis and Z. Iatridi, *Eur. Polym. J.*, 2011, **47**, 497.
34 (a) G. Gotzamanis and C. Tsitsilianis, *Macromol. Rapid Commun.*, 2006, **27,** 1757; (b) M. M. S. Lencina, Z. Iatridi, M. A. Villar and C. Tsitsilianis, *Eur. Polym. J.*, 2014, **61**, 33; (c) C. Charbonneau, C. Chassenieux, O. Colombani, and T. Nicolai, *Macromolecules*, 2011, **44**, 4487; (d) A. Shedge, O. Colombani, T. Nicolai and C. Chassenieux, *Macromolecules*, 2014, **47**, 2439.
35 H. Liu, Z. Guo, S. He, H. Yin, C. Fei and Y. Feng, *Polym. Chem.*, 2014, **5**, 4756.
36 H. Liu, Y. Zhao, C. A. Dreiss, Y. Feng, *Soft Matter*, 2014, **10**, 6387.
37 (a) Z. Cheng, X. Zhu, N. Zhou, J. Zhu and Z. Zhang, *Radiat. Phys. Chem.*, 2005, **72**, 695; (b) Y. Xu, Q. Xu, J. Lu,; X. Xia and L. Wang, *Polym. Bull.*, 2007, **58**, 809.
38 H. G. Shen and A. Eisenberg, *J. Am. Chem. Soc.*, 1999, **121**, 2728.
39 (a) J. Brandrup, E. H. Immergut, E. A. Grulke, A. Abe and D. R. Bloch, Polymer Handbook, 4th edition, *New York*, *Wiley*, 1999; (b) X. Li, H. Yang, L. Xu, X. Fu, H. Guo and X. Zhang, *Macromol. Chem. Phys.*, 2010, **211**, 297.
40 T. J. Martin, P. Munk and S. E. Webber, *Macromolecules*, 1996, **29**, 6071.
41 Z. Chu, C. A. Dreiss and Y. Feng, *Chem. Soc. Rev.*, 2013, **42**, 7174.
42 L. Sun, N. Petzetakis, A. Pitto-Barry, T. L. Schiller, N. Kirby, D. J. Keddie, B. J. Boyd, R. K. O'Reilly and A. P. Dove, *Macromolecules*, 2013, **46**, 9074.
43 T. Naolou, A. Meister, R. Schöps, M. Pietzsch and J. Kressler, *Soft Matter*, 2013, **9**, 10364.
44 X. Zhu and M. Liu, *Langmuir*, 2011, **27**, 12844.
45 C. Fernyhough, A. J. Ryan and G. Battaglia, *Soft Matter*, 2009, **5**, 1674.
46 (a) Y. Zhang, Y. Feng, J. Wang, S. He, Z. Guo, Z. Chu and C. A. Dreiss, *Chem. Commun.*, 2013, **49**, 4902; (b) Y. Zhang, Y. Feng, Y.Wang and X. Li, *Langmuir*, 2013, **29**, 4187.
47 (a) B. Li, X. Lu, Y. Ma and Z. Chen, *Eur. Polym. J.*, 2014, **60**, 255; (b) M. Satoh, E. Yoda, T. Hayashi and J. Komiyama, *Macromolecules*, 1989, **22**, 1808.
48 S. N. Sidorov, L. M. Bronstein, Y. A. Kabachii, P. M. Valetsky, P. L. Soo, D. Maysinger and A. Eisenberg, *Langmuir*, 2004, **20**, 3543.
49 E. Corradi, S. V. Meille, M. T. Messina, P. Metrangolo and G. Resnati, *Angew. Chem., Int. Ed.*, 2000, **112**, 1852.

**Table of content**